



# Event-triggered finite-time guaranteed cost control of asynchronous switched systems under the round-robin protocol via an AED-ADT method\*#

Hangli REN<sup>†1</sup>, Qingxi FAN<sup>1</sup>, Linlin HOU<sup>2</sup>

<sup>1</sup>School of Electric Information Engineering, Zhengzhou University of Light Industry, Zhengzhou 450000, China

<sup>2</sup>School of Information Science and Engineering, Qufu Normal University, Rizhao 276826, China

E-mail: renhangli2013@163.com; fqingxi520@163.com; houtingting8706@126.com

Received May 23, 2024; Revision accepted July 30, 2024; Crosschecked Aug. 26, 2024; Published online Oct. 17, 2024

**Abstract:** This paper focuses on addressing the problems of finite-time boundedness and guaranteed cost control in switched systems under asynchronous switching. To reduce redundant information transmission and alleviate data congestion of sensor nodes, two schemes are proposed: the event-triggered scheme (ETS) and the round-robin protocol (RRP). These schemes are designed to ensure that the system exhibits good dynamic characteristics while reducing communication resources. In the field of finite-time control, a switching signal is designed using the admissible edge-dependent average dwell time (AED-ADT) method. This method involves a slow AED-ADT switching and a fast AED-ADT switching, which are respectively suitable for finite-time stable and finite-time unstable situations of the controlled system within the asynchronous switching interval. By constructing a double-mode dependent Lyapunov function, the finite-time bounded criterion and the controller gain of the switched systems are obtained. Finally, the validity of the proposed results is showcased by implementing a buck-boost voltage circuit model.

**Key words:** Switched systems; Event-triggered scheme; Round-robin protocol; Asynchronous switching;

Admissible edge-dependent average dwell time (AED-ADT); Guaranteed cost control

<https://doi.org/10.1631/FITEE.2400427>

**CLC number:** TP13

## 1 Introduction

Because of the effective modeling approach provided by switching strategies for multi-mode control systems, the related control theories and methods of switched systems not only compensate for the shortcomings of single-mode control theory but also

provide theoretical references for general hybrid system research. Therefore, the research on switched systems has sparked the interest of many scholars (Huang et al., 2020; Karamanakos et al., 2021; Liu SL et al., 2022; Wang YD et al., 2022), particularly in the context of combined network transmission technology. In environments with restricted communication, complex network-induced factors such as network delay, data packet loss, and external interference often cause the system structure to exhibit different patterns. Clearly, in a multi-mode network and communication environment, a single system type and control strategy cannot be accurately modeled, making it difficult to achieve the expected control requirements. A multi-mode switching system driven by both time and events provides an effective

<sup>‡</sup> Corresponding author

\* Project supported by the Natural Science Foundation of Henan Province, China (No. 242300421175), the National Natural Science Foundation of China (No. 62003311), the China Postdoctoral Science Foundation (No. 2023M743191), the Key Scientific Research Projects of Higher Education Institutions in Henan Province, China (No. 24A120013), and the Natural Science Foundation of Shandong Province, China (No. ZR2023MF049)

# Electronic supplementary materials: The online version of this article (<https://doi.org/10.1631/FITEE.2400427>) contains supplementary materials, which are available to authorized users

ORCID: Hangli REN, <https://orcid.org/0000-0002-1809-7512>

© Zhejiang University Press 2024

theoretical foundation for addressing such issues. Integrating network transmission and switching technologies gives rise to networked switched systems, but such systems are not simply a superposition of these two. Although the introduction of switching technology presents unprecedented opportunities for solving complex and dynamic network control problems, it also creates obvious challenges, including data congestion, network delay, and asynchronous switching phenomena (Hu et al., 2016; Li et al., 2020; Xu et al., 2024).

To deal with the issue of redundant information transmission, event-triggered schemes (ETSs), with their unique “on-demand sampling” feature, have become an important method for improving data transmission rates (Dorf et al., 1962; Wakaiki and Sano, 2019; Li et al., 2020; Amini et al., 2021). In Qi et al. (2018), an ETS was proposed to solve the problem of finite-time control in networked switched systems. Due to the effects of quantization and packet loss, a periodic ETS was used to select specific events for applications in networked switched systems (Xiang and Johnson, 2017; Merlin et al., 2021). In Qi et al. (2019), the feedback signal from an improved periodic sampling ETS was used to study event-triggered control in switched systems with transmission delays. Based on sampled data information, a pattern-dependent event-triggered technique was established in Xie et al. (2022) to avoid Zeno behavior. It is worth noting that these results are based on the assumption that all sensors have simultaneous access to the transmission network for transmit signals, which is practically unlikely because network bandwidth is often limited.

In engineering practice, when multiple sensor nodes are simultaneously sending (or receiving) data over the network, it can lead to “data conflicts” and mutual interference of transmitted information, affecting the accuracy of transmission and even destroying the stability of the system. To address this issue, different types of communication protocols have been applied to avoid data conflicts (Liu K et al., 2015; Zou et al., 2017; Wan et al., 2019; Wang D et al., 2019; Mao et al., 2021). As a static protocol, the round-robin protocol (RRP) (Wen et al., 2016; Shang et al., 2022) has been widely used in industrial engineering security monitoring, computing scheduling, and so on because it is simple and easy to operate. Therefore, it is meaningful to adopt

a combination of ETS and RRP to deal with the problem of redundant information transmission and further solve the problem of data congestion in sensor nodes.

In network transmission technology, asynchronous switching phenomena are inevitable due to the influence of network delay on the modal signals of switched systems, and only being transmitted at discrete trigger points. When asynchronous phenomena exist but are not considered, the designed control strategies typically fail to achieve the expected system performance, and even the stability of the system cannot be guaranteed. Therefore, considering asynchronous phenomena in the analysis of switched systems is highly practical. In Li et al. (2020), the asynchronous event-triggered mechanism was considered from the sensor to the controller and from the controller to the actuator. Yang L et al. (2019) considered the asynchronous switching of system modes and filter modes that may occur within event intervals. The above literature generally assumes that the maximum asynchronous switching delay is known in advance, which has a certain level of conservatism. However, the admissible edge-dependent average dwell time (AED-ADT) (Yang JQ et al., 2018; Gao et al., 2020) method can study the system stability within asynchronous switching intervals, even when the maximum asynchronous interval is unknown.

In many studies of switched systems, most results are based on the analysis of their dynamic behavior within an infinite time interval. However, in practical applications, the transient performance of dynamic systems within specified time intervals is more valuable when studying systems with short working time, such as chemical reaction processes, satellite trajectory control systems, and furnace temperature control systems. The urgency to study the stability of systems within finite-time intervals leads to the concept of finite-time stability, which was first introduced by Weiss and Infante (1965). Since then, many related research results have emerged (Muresan and Liu, 2019, 2022; Sun et al., 2021). It is noted that the AED-ADT switching signal design method is rarely used for finite-time control of the switched system. Compared to the mode-dependent average dwell time (MDADT) method (Du et al., 2022), this method not only uses the current subsystems’ mode signals but also leverages previous

mode signals to effectively use the system's mode information for studying transient characteristics. Therefore, applying the AED-ADT design method to finite-time control problems is meaningful, which is another motivation of this work.

Motivated by the above observations, this study addresses the issues of finite-time boundedness and guaranteed cost control in asynchronous switched systems under ETS and RRP. The contributions of this paper are summarized as follows:

1. A joint ETS and RRP design method is proposed, which ensures good data filtering while avoiding sensor node congestion.
2. In switching signal design that takes into account the significance of finite-time control, the method with modal memory, namely AED-ADT, is applied. This method better reflects the switching characteristics of modal signals.
3. By implementing slow AED-ADT switching and fast AED-ADT switching techniques, the challenges of finite-time instability in the controlled system during asynchronous switching intervals are addressed, thereby diminishing the impact of unstable conditions on the control system and ensuring finite-time stability.
4. Based on RRP and ETS, sufficient criteria are obtained to ensure the finite-time boundedness of the switched system and the establishment of the guaranteed cost control index.

Notations: In this paper,  $\mathbb{R}^l$  denotes the set of  $l$ -dimensional real vectors,  $\mathbb{N}$  the set of natural numbers, and  $\lambda_m(\mathbf{P})(\lambda_M(\mathbf{P}))$  the minimum (maximum) eigenvalue of matrix  $\mathbf{P}$ .  $\mathbf{I}_n$  and  $\mathbf{0}_n$  denote the  $n \times n$  identity matrix and  $n \times n$  zero matrix, respectively.  $\mathbf{P}^T$  and  $\mathbf{P}^{-1}$  stand for the transpose and inverse of  $\mathbf{P}$ , respectively. The block-diagonal matrix of  $\mathbf{P}_1$  and  $\mathbf{P}_2$  is represented by  $\text{diag}\{\mathbf{P}_1, \mathbf{P}_2\}$ .  $\lceil \cdot \rceil$  stands for rounding up to an integer.  $\text{col}\{\cdot\}$  denotes the column vector.

## 2 Problem formulation

### 2.1 System description

The following system is given:

$$\dot{\mathbf{x}}(t) = \mathbf{A}_{\sigma(t)}\mathbf{x}(t) + \mathbf{B}_{\sigma(t)}\mathbf{u}(t) + \mathbf{E}_{\sigma(t)}\boldsymbol{\omega}(t), \quad (1)$$

where  $\mathbf{x}(t) \in \mathbb{R}^l$  is the state,  $\mathbf{u}(t) \in \mathbb{R}^m$  is the input, and the disturbance is  $\boldsymbol{\omega}(t) \in \mathbb{R}^m$ . The switching

law is denoted as  $\sigma(t) \in [0, \infty) \rightarrow \mathcal{W} = \{1, 2, \dots, s\}$ . The switched sequence set is denoted by  $\{t_h, \sigma(t_h)\}$ , and the switched points  $t_h$  satisfy  $0 < t_1 < \dots < t_h < \dots, h \in \mathbb{N}$ . When  $t \in [t_h, t_{h+1})$ , the  $\sigma(t_h)$ - $t_h$  subsystem is activated.  $\mathbf{A}_i, \mathbf{B}_i$ , and  $\mathbf{E}_i$  ( $i \in \mathcal{W}$ ) are known matrices of real constant.

**Remark 1** The system model (1) describes a typical multi-mode switched system. Multi-mode switching is an effective modeling and analysis technique. Many practical systems involve controlled objects that can be described as multi-mode switching control systems; for example, DC-DC converters in power systems can obtain the required voltage by switching to different paths (here, DC is short for direct current); unmanned helicopters switch between flight modes such as hovering, forward flight, turning, climbing, descending, and diving; Bang-Bang control is used to solve the optimal fuel problems in the aerospace field.

Taking into account the impacts of event-triggered sampling and network transmission delays, the modes of the controller often do not align with the switching pace of the system, resulting in asynchronous switching. Without loss of generality,  $\varrho(t)$  is used here to denote the controller's modal signal. Then, a state feedback controller  $\mathbf{u}(t) = \mathbf{K}_{\varrho(t)}\mathbf{x}(t)$  based on asynchronous switching characteristics is designed for system (1), and  $\mathbf{K}_{\varrho(t)}$  indicates the controller gain to be designed.

### 2.2 ETS and RRP design

As shown in Fig. 1, ETS and RRP are introduced to reduce the network transmission frequency and alleviate the transmission load of the sensor nodes.

**Remark 2** Fig. 1 illustrates that due to the promiscuity and particularity of the switched system itself, the introduction of RRP, ETS, and network transmission technology has increased the complexity of the closed-loop control system structure because it contains not only the switching features of the switched system but also the node data switching features under the action of the scheduling protocol. Specifically, to reduce the transmission frequency, triggered data packet  $(\mathbf{x}(g_c k), \sigma(g_c k))$  is transmitted to the controller only at discrete trigger point  $t = g_c k$  through the network. Therefore, the switching instants of the mode-dependent controller will be out of sync with the switched systems, i.e.,  $\sigma(t) \neq \varrho(t)$ .

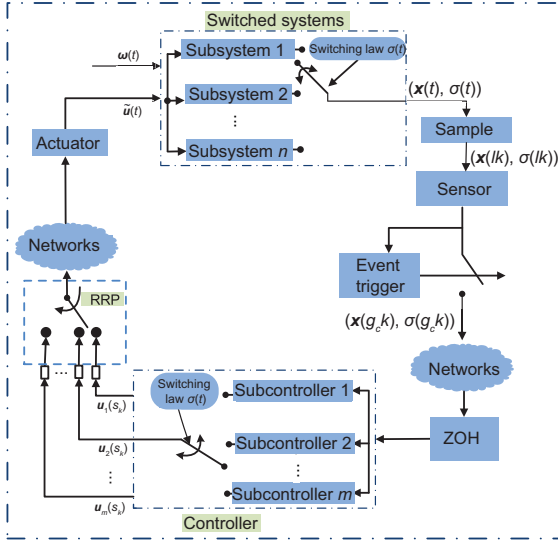


Fig. 1 Structure of a closed-loop switched system

According to the RRP-based control structure, only one node at a time is allowed to obtain permission to use the communication network and transmit the corresponding data, thus reducing the transmission load of sensor nodes.

To avoid Zeno phenomenon, a discrete ETS is introduced here; that is, system (1) is first sampled with a fixed period  $k$  ( $< \tau_{a,b}$ ), where  $\tau_{a,b}$  indicates the interval between two adjacent switching points. Then, a hybrid ETS is designed to further screen the periodically sampled data to reduce the transmission rate of redundant information, as follows:

$$\begin{aligned}
 &g_{c+1}k \\
 &= g_c k + \min_{v \in \mathbb{N}} \{vk | e^T((g_c+v)k) \Phi_{\sigma(s_{c,v}k)} e((g_c+v)k) \\
 &\geq \partial(s_{c,v}k) \mathbf{x}^T((g_c+v)k) \Phi_{\sigma(s_{c,v}k)} \mathbf{x}((g_c+v)k)\}, \quad (2)
 \end{aligned}$$

where  $e((g_c+v)k) = \mathbf{x}((g_c+v)k) - \mathbf{x}(g_c k)$ ,  $s_{c,v}k \triangleq (g_c+v)k$  is the sampling instant in  $[g_c k, g_{c+1}k)$ ,  $v \in \mathbb{N}$ ,  $\Phi_{\sigma(s_{c,v}k)} > 0$  is a weighting matrix, and  $\partial(s_{c,v}k)$  is the coefficient of the threshold (when  $s_{c,v}k = \lceil \frac{t_h}{k} \rceil k$ , then  $\partial(s_{c,v}k) = 0$ , and  $\partial(s_{c,v}k) > 0$  otherwise).

**Remark 3** From Eq. (2), it is not difficult to see that when  $s_{c,v}k = \lceil \frac{t_h}{k} \rceil k$ , then  $\partial(s_{c,v}k) = 0$ , and data packet  $(\mathbf{x}(\lceil \frac{t_h}{k} \rceil k), \sigma(\lceil \frac{t_h}{k} \rceil k))$  must be triggered at  $\lceil \frac{t_h}{k} \rceil k$ , which is the minimum sampling time at the right of the switching point  $t_h$  (including  $t_h$ ).

Because the communication load is generated

in the transmission channel between the controller and the actuator, it is necessary to design an RRP to regulate sensor communication to prevent data collisions. According to the RRP, we have  $\iota([t]) = \text{mod}([t] - 1, \psi) + 1, \forall t \in [0, \infty)$ , where  $\psi \in \{1, 2, \dots, \Psi\}$ ,  $\iota([t])$  is the network node that is transmitted at time  $t$ , and  $[t]$  is the smallest positive integer greater than  $t$ . Let  $\tilde{\mathbf{u}}(t) = [\tilde{u}_1(t), \tilde{u}_2(t), \dots, \tilde{u}_m(t)]$  represent the signal transmitted by the controller over the network.

The updated rule for  $\tilde{\mathbf{u}}_\ell(t)$  is designed: if  $\ell = \iota([t])$ , then  $\tilde{\mathbf{u}}_\ell(t) = \tilde{\mathbf{u}}_\ell(g_c k)$ , and  $\tilde{\mathbf{u}}_\ell(t) = \mathbf{0}$  otherwise. Then, we have

$$\begin{aligned}
 \tilde{\mathbf{u}}(t) &= \Lambda_\ell \mathbf{u}(g_c k) = \Lambda_\ell \mathbf{K}_{\sigma(g_c k)} \mathbf{x}(g_c k), \\
 t &\in [g_c k + \tau_{g_c}, g_{c+1}k + \tau_{g_{c+1}}), \quad (3)
 \end{aligned}$$

where  $\Lambda_\ell = \text{diag}\{\tilde{\delta}_\ell^1, \tilde{\delta}_\ell^2, \dots, \tilde{\delta}_\ell^m\}$  and  $\tilde{\delta}_m^n = \delta(n - m)$  is the Kronecker delta function.

**Remark 4** In dual-network transmission model, the time delay  $\tau_{g_c}$  of the network channel mainly consists of two parts: (1)  $\tau_{g_c}^s$  is the transmission delay when the triggering signal is transmitted to the controller through the network channel; (2)  $\tau_{g_c}^a$  is the transmission delay when the control signal passing through the RRP is transmitted to the actuator through the network channel. That is to say,  $\tau_{g_c} \triangleq \tau_{g_c}^s + \tau_{g_c}^a$ , which is assumed to satisfy  $\tau_m \leq \tau_{g_c} \leq \tau_M < k$ .

**Remark 5** With the trigger action,  $(\mathbf{x}(g_c k), \sigma(g_c k))$  is the input signal of the controller instead of  $(\mathbf{x}(t), \sigma(t))$ , which can remain unchanged until new triggered data packets arrive. Therefore,  $\varrho(t) = \sigma(g_c k), t \in [g_c k + \tau_{g_c}, g_{c+1}k + \tau_{g_{c+1}})$ .

Next, to conveniently describe the periodic sampling information within the triggering interval, the signal holding interval  $[g_c k + \tau_{g_c}, g_{c+1}k + \tau_{g_{c+1}}]$  is divided into several subintervals:

$$[g_c k + \tau_{g_c}, g_{c+1}k + \tau_{g_{c+1}}) = \bigcup_{v=0}^{l_c} \Gamma_{c,v}, \quad (4)$$

where  $\Gamma_{c,v} = [s_{c,v}k + \tau_{s_{c,v}}, s_{c,v+1}k + \tau_{s_{c,v+1}})$  and  $l_c = g_{c+1} - g_c - 1$ . The invisible time delay  $\tau_{s_{c,v}}$  satisfies  $\tau_m \leq \tau_{s_{c,v}} \leq \tau_M \leq k$  and  $s_{c,v}k + \tau_{s_{c,v}} < s_{c,v+1}k + \tau_{s_{c,v+1}}$ .

Define  $\varepsilon(t) = t - s_{c,v}k, \varepsilon_m \leq \varepsilon(t) \leq \varepsilon_M, \varepsilon_m = \tau_m$ , and  $\varepsilon_M = \tau_M + k$ . Then, combined with ETS and RRP, system (1) can be reconstituted as Eq. (5):

$$\begin{cases} \dot{\mathbf{x}}(t) = \mathbf{A}_{\sigma(t)} \mathbf{x}(t) + \tilde{\mathbf{B}}_{\sigma(t)} \mathbf{K}_{\sigma(t)} \mathbf{x}(t - \varepsilon(t)) - \tilde{\mathbf{B}}_{\sigma(t)} \mathbf{K}_{\sigma(t)} e(s_{c,v}k) + \mathbf{E}_{\sigma(t)} \boldsymbol{\omega}(t), & t \in T_s[t_h, t_{h+1}), \\ \dot{\mathbf{x}}(t) = \mathbf{A}_{\sigma(t)} \mathbf{x}(t) + \tilde{\mathbf{B}}_{\sigma(t)} \mathbf{K}_{\varrho(t)} \mathbf{x}(t - \varepsilon(t)) - \tilde{\mathbf{B}}_{\sigma(t)} \mathbf{K}_{\varrho(t)} e(s_{c,v}k) + \mathbf{E}_{\sigma(t)} \boldsymbol{\omega}(t), & t \in T_u[t_h, t_{h+1}). \end{cases} \quad (5)$$

$T_s[t_h, t_{h+1})$  and  $T_u[t_h, t_{h+1})$  denote the synchronous switching interval and the asynchronous switching interval respectively,  $\mathbf{x}(\varsigma) = \phi(\varsigma)$ ,  $\varsigma \in [-\varepsilon_M, 0]$ , and  $\tilde{\mathbf{B}}_{\sigma(t)} \triangleq \mathbf{B}_{\sigma(t)} \mathbf{A}_\ell$ .

**Remark 6** Due to the mismatch between the controller and system modes, the controlled system may be finite-time unstable during asynchronous control. Therefore, the transient performance of the controlled system in the asynchronous switching interval  $T_u[t_h, t_{h+1})$  will be discussed in two cases, i.e, finite-time stable and finite-time unstable. For brevity,  $T_{u\downarrow}[t_h, t_{h+1})$  represents the finite-time stable interval and  $T_{u\uparrow}[t_h, t_{h+1})$  represents the finite-time unstable interval.

**Definition 1** (Branicky, 1998) Given switching signal  $\sigma$  and  $n, m \rightarrow \mathcal{W}$  ( $n \neq m$ ),  $T_{n,m}(t_h, t_{h+1})$  indicates the total runtime of subsystem  $n$  in  $[t_h, t_{h+1})$  and  $N_{n,m}^\sigma(t_h, t_{h+1})$  indicates the number of times that subsystem  $n$  switches to subsystem  $m$ . Based on this,  $\sigma(t)$  has a slow AED-ADT  $\tau_{n,m}^a$  and a fast AED-ADT  $d_{n,m}^a$ . If there are nonnegative numbers  $\underline{N}_{n,m}^0, \overline{N}_{n,m}^0$  and  $\tau_{n,m}^a, d_{n,m}^a$ , then the following inequalities hold:

$$N_{n,m}^\sigma \leq \underline{N}_{n,m}^0 + \frac{T_{n,m}(t_h, t_{h+1})}{\tau_{n,m}^a}, \forall t_{h+1} \geq t_h \geq 0, \quad (6)$$

$$N_{n,m}^\sigma \geq \overline{N}_{n,m}^0 + \frac{T_{n,m}(t_h, t_{h+1})}{d_{n,m}^a}, \forall t_{h+1} \geq t_h \geq 0, \quad (7)$$

where  $\underline{N}_{n,m}^0$  and  $\overline{N}_{n,m}^0$  are called AED chatter bounds.

**Remark 7** Due to the existence of unmatched time periods, the transient characteristics of the system may be affected, and even lead to finite-time instability. For this situation, the switching strategy will be adopted as follows: when the activated subsystem is finite-time stable, the slow AED-ADT method can be used to design the switching signal of the system; otherwise, the fast AED-ADT method will be adopted to make the switched system achieve finite-time stability as soon as possible.

**Definition 2** (Branicky, 1998) Given matrix  $\mathbf{R} > 0$ , two scalars  $c_2 > c_1 > 0$ , and an integer  $T_f > 0$ , the switched system (1) is finite-time bounded with respect to  $(\mathbf{R}, T_f, c_1, c_2)$ , if

$$\begin{aligned} & \max_{\varsigma \in [-\varepsilon_M, 0]} \{ \mathbf{x}^T(\varsigma) \mathbf{R} \mathbf{x}(\varsigma), \dot{\mathbf{x}}^T(\varsigma) \mathbf{R} \dot{\mathbf{x}}(\varsigma) \} \leq c_1 \\ & \Rightarrow \mathbf{x}^T(t) \mathbf{R} \mathbf{x}(t) \leq c_2. \end{aligned} \quad (8)$$

**Assumption 1** Given a positive integer  $T_f, \forall t \in$

$[0, T_f]$ , the external signal  $\boldsymbol{\omega}(t)$  satisfies

$$\int_0^{T_f} \boldsymbol{\omega}^T(\rho) \boldsymbol{\omega}(\rho) d\rho \leq d, \quad (9)$$

where  $d$  is a positive constant.

**Problem** For the given switched system (1), our main task is to realize the cooperative design of asynchronous switching strategy, ETS, and RRP, so that

- (1) the augmented system (5) is finite-time bounded (FTB) with respect to  $(\mathbf{R}, T_f, c_1, c_2)$ , and
- (2) under the zero initial condition, the augmented system (5) satisfies

$$J = \int_0^{T_f} [\mathbf{x}^T(t) \mathbf{Q}_{\sigma(t)} \mathbf{x}(t) dt + \mathbf{u}^T(t) \mathbf{D}_{\sigma(t)} \mathbf{u}(t) dt] < J^*, \quad (10)$$

where  $J^*$  is a constant,  $\sigma(t) \in \mathcal{W}$ , matrix  $\mathbf{Q}_{\sigma(t)} > 0$ , and  $\mathbf{D}_{\sigma(t)} > 0$ .

### 3 Main results

#### 3.1 FTB analysis under the guaranteed cost controller

**Theorem 1** Given positive scalars  $c_1, c_2$  ( $c_2 \geq c_1$ ),  $k, \varrho_0, \varepsilon_m, \varepsilon_M, d, T_f$ , and matrix  $\mathbf{R} > 0$ , for values  $\alpha_i > 0$  with  $0 < v_{i,j} < 1, (i, j) \in \Theta_s, \gamma_{i,j} > 0$  with  $0 < \mu_{i,j} < 1, (i, j) \in \Theta_{u\downarrow}$ , and  $\gamma_{i,j} < 0$  with  $\mu_{i,j} > 1, (i, j) \in \Theta_{u\uparrow}$ , the event-based asynchronous control loop system (5) is FTB with respect to  $(\mathbf{R}, T_f, c_1, c_2)$  and the cost function  $J$  satisfies  $J < J^*$ , if there exist matrices  $\Phi_i > 0, \mathbf{P}_i > 0, \mathbf{H}_i^i > 0, \mathbf{M}_i^j > 0, (i, j) \in \Theta_s$ , and  $T_{i,j}, \mathbf{K}_i, \mathbf{P}_{i,j} > 0, \mathbf{H}_{i,j}^i > 0, \mathbf{M}_{i,j}^j > 0, (i, j) \in \Theta_u, j, i = 1, 2, \forall i, j \in \mathcal{W}, i \neq j$ , such that

$$\begin{bmatrix} \mathbf{U}_0 & \mathbf{U}_1 \\ * & \mathbf{U}_2 \end{bmatrix} < 0, \quad (11)$$

$$\begin{bmatrix} \Xi_0 & \Xi_1 \\ * & \Xi_2 \end{bmatrix} < 0, \quad (12)$$

$$\begin{bmatrix} \mathbf{M}_i^2 & \mathbf{Z}_i \\ \mathbf{Z}_i^T & \mathbf{M}_i^2 \end{bmatrix} > 0, \quad (13)$$

$$\begin{bmatrix} \mathbf{M}_{i,j}^2 & \mathbf{Z}_{i,j} \\ \mathbf{Z}_{i,j}^T & \mathbf{M}_{i,j}^2 \end{bmatrix} > 0, \quad (14)$$

$$\mathbf{P}_{i,j} \leq \mu_{i,j} \mathbf{P}_{j,j}, \mathbf{H}_{i,j}^i \leq \mu_{i,j} \mathbf{H}_{j,j}^i, \mathbf{M}_{i,j}^j \leq \mu_{i,j} \mathbf{M}_{j,j}^j, \quad (15)$$

$$\mathbf{P}_i \leq v_{i,j} \mathbf{P}_{i,j}, \mathbf{H}_i^i \leq v_{i,j} \mathbf{H}_{i,j}^i, \mathbf{M}_i^j \leq v_{i,j} \mathbf{M}_{i,j}^j, \quad (16)$$



$$\begin{cases} (\vartheta_i + d)e^{\xi_{i,j}} < c_2\lambda_1, \\ (\vartheta_i + d)e^{\bar{\xi}_{i,j}} < c_2\lambda_1, \\ (\vartheta_i + d)e^{\bar{\xi}_{i,j}} > c_2\lambda_1, \end{cases} \quad (17)$$

$$\begin{aligned} \tau_{i,j}^a &\geq (\tau_{i,j}^a)^* \\ &= \frac{T_{i,j} \ln v_{i,j}}{\ln(c_2\lambda_1) - \ln(\vartheta_i + d) - \xi_{i,j}}, \quad (i, j) \in \Theta_s, \end{aligned} \quad (18)$$

$$\begin{aligned} d_{i,j}^a &\geq (d_{i,j}^a)^* \\ &= \frac{T_{i,j} \ln \mu_{i,j}}{\ln(c_2\lambda_1) - \ln(\vartheta_i + d) - \bar{\xi}_{i,j}}, \quad (i, j) \in \Theta_{u\downarrow}, \end{aligned} \quad (19)$$

$$\begin{aligned} d_{i,j}^a &\leq (d_{i,j}^a)^* \\ &= \frac{T_{i,j} \ln \mu_{i,j}}{\ln(c_2\lambda_1) - \ln(\vartheta_i + d) - \bar{\xi}_{i,j}}, \quad (i, j) \in \Theta_{u\uparrow}, \end{aligned} \quad (20)$$

where

$$\mathfrak{U}_0 = \begin{bmatrix} \mathfrak{U}(11) & \mathfrak{U}(12) & M_i^1 & \mathbf{0} & P_i E_i & \mathfrak{U}(16) & \mathbf{0} \\ * & \mathfrak{U}(22) & \mathfrak{U}(23) & \mathfrak{U}(24) & \mathbf{0} & \mathbf{0} & K_i^T \\ * & * & \mathfrak{U}(33) & e^{\alpha_i \varepsilon_m} Z_i & \mathbf{0} & \mathbf{0} & \mathbf{0} \\ * & * & * & \mathfrak{U}(44) & \mathbf{0} & \mathbf{0} & \mathbf{0} \\ * & * & * & * & -I & \mathbf{0} & \mathbf{0} \\ * & * & * & * & * & -\Phi_i & -K_i^T \\ * & * & * & * & * & * & -D_i^{-1} \end{bmatrix}, \quad (21)$$

$$\mathfrak{U}_1 = \begin{bmatrix} \varepsilon_m A_i^T & (\varepsilon_M - \varepsilon_m) A_i^T \\ \varepsilon_m K_i^T \tilde{B}_i^T & (\varepsilon_M - \varepsilon_m) K_i^T \tilde{B}_i^T \\ \mathbf{0} & \mathbf{0} \\ \mathbf{0} & \mathbf{0} \\ \varepsilon_m E_i & (\varepsilon_M - \varepsilon_m) E_i \\ -\varepsilon_m K_i^T \tilde{B}_i^T & -(\varepsilon_M - \varepsilon_m) K_i^T \tilde{B}_i^T \\ \mathbf{0} & \mathbf{0} \end{bmatrix}, \quad (22)$$

$$\mathfrak{U}_2 = \text{diag}\{M_i^{-1}, M_i^{-2}\}, \quad (23)$$

$$\mathfrak{E}_0 = \begin{bmatrix} \mathfrak{E}(11) & \mathfrak{E}(12) & M_{i,j}^1 & \mathbf{0} & P_{i,j} E_i & \mathfrak{E}(16) & \mathbf{0} \\ * & \mathfrak{E}(22) & \mathfrak{E}(23) & \mathfrak{E}(24) & \mathbf{0} & \mathbf{0} & K_j^T \\ * & * & \mathfrak{E}(33) & e^{\gamma_{i,j} \varepsilon_m} Z_{i,j} & \mathbf{0} & \mathbf{0} & \mathbf{0} \\ * & * & * & \mathfrak{E}(44) & \mathbf{0} & \mathbf{0} & \mathbf{0} \\ * & * & * & * & -I & \mathbf{0} & \mathbf{0} \\ * & * & * & * & * & -\Phi_j & -K_j^T \\ * & * & * & * & * & * & -D_{i,j}^{-1} \end{bmatrix}, \quad (24)$$

$$\mathfrak{E}_1 = \begin{bmatrix} \varepsilon_m A_i^T & (\varepsilon_M - \varepsilon_m) A_i^T \\ \varepsilon_m K_j^T \tilde{B}_i^T & (\varepsilon_M - \varepsilon_m) K_j^T \tilde{B}_i^T \\ \mathbf{0} & \mathbf{0} \\ \mathbf{0} & \mathbf{0} \\ \varepsilon_m E_i & (\varepsilon_M - \varepsilon_m) E_i \\ -\varepsilon_m K_j^T \tilde{B}_i^T & -(\varepsilon_M - \varepsilon_m) K_j^T \tilde{B}_i^T \\ \mathbf{0} & \mathbf{0} \end{bmatrix}, \quad (25)$$

$$\mathfrak{E}_2 = \text{diag}\{M_{i,j}^{-1}, M_{i,j}^{-2}\}, \quad (26)$$

$$\mathfrak{U}(11) = A_i^T P_i + P_i A_i + H_i^1 - \alpha_i P_i - M_i^1 + Q_i, \quad (27)$$

$$\mathfrak{U}(12) = P_i \tilde{B}_i K_i, \quad (28)$$

$$\mathfrak{U}(16) = -P_i \tilde{B}_i K_i, \quad (29)$$

$$\mathfrak{U}(22) = -e^{\alpha_i \varepsilon_m} (2M_i^2 - Z_i - Z_i^T) + \partial_i \Phi_i, \quad (30)$$

$$\mathfrak{U}(23) = e^{\alpha_i \varepsilon_m} (M_i^2 - Z_i^T), \quad (31)$$

$$\mathfrak{U}(24) = e^{\alpha_i \varepsilon_m} (M_i^2 - Z_i), \quad (32)$$

$$\mathfrak{U}(33) = e^{\alpha_i \varepsilon_m} (H_i^2 - H_i^1 - M_i^2) - M_i^1, \quad (33)$$

$$\mathfrak{U}(44) = e^{\alpha_i \varepsilon_m} H_i^2 - e^{\alpha_i \varepsilon_m} M_i^2, \quad (34)$$

$$\mathfrak{E}(11) = A_i^T P_{i,j} + P_{i,j} A_i + H_{i,j}^1 - \gamma_{i,j} P_{i,j} - M_{i,j}^1 + Q_{i,j}, \quad (35)$$

$$\mathfrak{E}(12) = P_{i,j} \tilde{B}_i K_j, \quad (36)$$

$$\mathfrak{E}(16) = -P_{i,j} \tilde{B}_i K_j, \quad (37)$$

$$\mathfrak{E}(22) = -e^{\gamma_{i,j} \varepsilon_m} (2M_{i,j}^2 - Z_{i,j} - Z_{i,j}^T) + \partial_j \Phi_j, \quad (38)$$

$$\mathfrak{E}(23) = e^{\gamma_{i,j} \varepsilon_m} (M_{i,j}^2 - Z_{i,j}^T), \quad (39)$$

$$\mathfrak{E}(24) = e^{\gamma_{i,j} \varepsilon_m} (M_{i,j}^2 - Z_{i,j}), \quad (40)$$

$$\mathfrak{E}(33) = e^{\gamma_{i,j} \varepsilon_m} (H_{i,j}^2 - H_{i,j}^1 - M_{i,j}^2) - M_{i,j}^1, \quad (41)$$

$$\mathfrak{E}(44) = e^{\gamma_{i,j} \varepsilon_m} H_{i,j}^2 - e^{\gamma_{i,j} \varepsilon_m} M_{i,j}^2, \quad (42)$$

$$P_i = R^{\frac{1}{2}} \hat{P}_i R^{\frac{1}{2}}, \quad (43)$$

$$H_i^1 = R^{\frac{1}{2}} \hat{H}_i^1 R^{\frac{1}{2}}, \quad (44)$$

$$M_i^j = R^{\frac{1}{2}} \hat{M}_i^j R^{\frac{1}{2}}, \quad (45)$$

$$\lambda_1 = \lambda_M(\hat{P}_i), \quad (46)$$

$$\lambda_2 = \max\{\lambda_M(\hat{P}_i), \lambda_M(\hat{H}_i^1), \lambda_M(\hat{M}_i^j)\}, \quad (47)$$

$$\begin{cases} \xi_{i,j} = \underline{N}_{i,j}^0 \ln v_{i,j} + \alpha_i T_{i,j}, \\ \bar{\xi}_{i,j} = \bar{N}_{i,j}^0 \ln \mu_{i,j} + \gamma_{i,j} T_{i,j}. \end{cases} \quad (48)$$

The proof of Theorem 1 is provided in the supplementary materials.

### 3.2 Asynchronous guaranteed cost controller design

**Theorem 2** Given positive scalars  $c_1, c_2$  ( $c_2 \geq c_1$ ),  $k, \varrho_0, \varepsilon_m, \varepsilon_M, d, T_f$ , and matrix  $R > 0$ , for values  $\alpha_i > 0$  with  $0 < v_{i,j} < 1, (i, j) \in \Theta_s, \gamma_{i,j} > 0$  with  $0 < \mu_{i,j} < 1, (i, j) \in \Theta_{u\downarrow}$ , and  $\gamma_{i,j} < 0$  with  $\mu_{i,j} > 1, (i, j) \in \Theta_{u\uparrow}$ , if there exist matrices  $S_i > 0, \tilde{\Phi}_i > 0, \hat{P}_i > 0, \hat{H}_i^1 > 0, \hat{M}_i^j > 0, (i, j) \in \Theta_s, \tilde{\Phi}_j > 0, \hat{P}_{i,j} > 0, \hat{H}_{i,j}^1 > 0, \hat{M}_{i,j}^j > 0, (i, j) \in \Theta_{u\downarrow}, i, j \in \{1, 2\}$ , and real matrices  $Y_i, \tilde{Z}_i, \tilde{Z}_{i,j}, \forall i, j \in \mathcal{W}$  ( $i \neq j$ ), such that inequality (18) and the

following inequalities hold:

$$\begin{bmatrix} \check{U}_{11} & \check{U}_{12} \\ * & \check{U}_{22} \end{bmatrix} < 0, \tag{49}$$

$$\begin{bmatrix} \check{\Xi}_0 & \check{\Xi}_1 \\ * & \check{\Xi}_2 \end{bmatrix} < 0, \tag{50}$$

$$\begin{bmatrix} \check{M}_i^2 & \check{Z}_i \\ \check{Z}_i^T & \check{M}_i^2 \end{bmatrix} > 0, \tag{51}$$

$$\begin{bmatrix} \check{M}_{i,j}^2 & \check{Z}_{i,j} \\ \check{Z}_{i,j}^T & \check{M}_{i,j}^2 \end{bmatrix} > 0, \tag{52}$$

$$\check{P}_i \leq v_{i,j} \check{P}_{i,j}, \check{H}_i^1 \leq v_{i,j} \check{H}_{i,j}^1, \check{M}_i^1 \leq v_{i,j} \check{M}_{i,j}^1, \tag{53}$$

$$\check{P}_{i,j} \leq \mu_{i,j} \check{P}_j, \check{H}_{i,j}^1 \leq \mu_{i,j} \check{H}_j^1, \check{M}_{i,j}^1 \leq \mu_{i,j} \check{M}_j^1, \tag{54}$$

then the augmented system (5) is FTB with respect to  $(R, T_f, c_1, c_2)$  and the performance index  $J^*$  can be obtained. Moreover, the admissible controller gain is given by  $K_i = Y_i S_i^{-1}$ .

Here are the expressions of the symbols:

$$\check{U}_{12} = \begin{bmatrix} \mathbf{0} & \mathbf{0} \\ \varepsilon_m S_i^T A_i^T & (\varepsilon_M - \varepsilon_m) S_i^T A_i^T \\ \varepsilon_m Y_i^T \tilde{B}_i^T & (\varepsilon_M - \varepsilon_m) Y_i^T \tilde{B}_i^T \\ \mathbf{0} & \mathbf{0} \\ \mathbf{0} & \mathbf{0} \\ \varepsilon_m E_i & (\varepsilon_M - \varepsilon_m) E_i \\ -\varepsilon_m Y_i^T \tilde{B}_i^T & -(\varepsilon_M - \varepsilon_m) Y_i^T \tilde{B}_i^T \\ \mathbf{0} & \mathbf{0} \end{bmatrix}. \tag{56}$$

$$\check{U}_{22} = \text{diag}\{\check{M}_i^1 - 2S_i, \check{M}_i^2 - 2S_i\}. \tag{57}$$

$$\check{\Xi}_1 = \begin{bmatrix} \mathbf{0} & \mathbf{0} \\ \varepsilon_m S_j^T A_i^T & (\varepsilon_M - \varepsilon_m) S_j^T A_i^T \\ \varepsilon_m Y_j^T \tilde{B}_i^T & (\varepsilon_M - \varepsilon_m) Y_j^T \tilde{B}_i^T \\ \mathbf{0} & \mathbf{0} \\ \mathbf{0} & \mathbf{0} \\ \varepsilon_m E_i & (\varepsilon_M - \varepsilon_m) E_i \\ -\varepsilon_m Y_j^T \tilde{B}_i^T & -(\varepsilon_M - \varepsilon_m) Y_j^T \tilde{B}_i^T \\ \mathbf{0} & \mathbf{0} \end{bmatrix}. \tag{59}$$

$$\check{\Xi}_2 = \text{diag}\{\check{M}_{i,j}^1 - 2S_j, \check{M}_{i,j}^2 - 2S_j\}. \tag{60}$$

$$\check{U}_{01} = -\alpha_i \check{P}_i + \check{H}_i^1 - \check{M}_i^1 + \check{Q}_i. \tag{61}$$

$$\check{U}(33) = -e^{\alpha_i \varepsilon_m} (2\check{M}_i^2 - \check{Z}_i - \check{Z}_i^T) + \partial_i \check{\Phi}_i. \tag{62}$$

$$\check{U}(34) = e^{\alpha_i \varepsilon_m} (\check{M}_i^2 - \check{Z}_i^T). \tag{63}$$

$$\check{U}(35) = e^{\alpha_i \varepsilon_m} (\check{M}_i^2 - \check{Z}_i). \tag{64}$$

$$\check{U}(44) = e^{\alpha_i \varepsilon_m} (\check{H}_i^2 - \check{H}_i^1 - \check{M}_i^2) - \check{M}_i^1. \tag{65}$$

$$\check{U}(55) = e^{\alpha_i \varepsilon_M} \check{H}_i^2 - e^{\alpha_i \varepsilon_m} \check{M}_i^2. \tag{66}$$

$$\check{\Xi}_{01} = -\gamma_{i,j} \check{P}_{i,j} + \check{H}_{i,j}^1 - \check{M}_{i,j}^1 + \check{Q}_{i,j}. \tag{67}$$

$$\check{\Xi}(33) = -e^{\gamma_{i,j} \varepsilon_m} (2\check{M}_{i,j}^2 - \check{Z}_{i,j} - \check{Z}_{i,j}^T) + \partial_j \check{\Phi}_j. \tag{68}$$

$$\check{\Xi}(44) = e^{\gamma_{i,j} \varepsilon_m} (\check{H}_{i,j}^2 - \check{H}_{i,j}^1 - \check{M}_{i,j}^2) - \check{M}_{i,j}^1. \tag{69}$$

$$\check{\Xi}(34) = e^{\gamma_{i,j} \varepsilon_m} (\check{M}_{i,j}^2 - \check{Z}_{i,j}^T). \tag{70}$$

$$\check{\Xi}(35) = e^{\gamma_{i,j} \varepsilon_m} (\check{M}_{i,j}^2 - \check{Z}_{i,j}). \tag{71}$$

$$\check{\Xi}(55) = e^{\gamma_{i,j} \varepsilon_M} \check{H}_{i,j}^2 - e^{\gamma_{i,j} \varepsilon_m} \check{M}_{i,j}^2. \tag{72}$$

**Proof** Define  $S_i = X_i^{-1}, Y_i = K_i S_i, \check{P}_i = S_i^T P_i S_i, \check{Q}_i = S_i^T Q_i S_i, \check{Q}_{i,j} = S_i^T Q_{i,j} S_i, \check{D}_i = S_i^T D_i S_i, \check{H}_i^1 = S_i^T H_i S_i, \check{M}_i^1 = S_i^T M_i^1 S_i, \check{P}_{i,j} = S_i^T P_{i,j} S_i, \check{D}_{i,j} = S_i^T D_{i,j} S_i, \check{H}_{i,j}^1 = S_i^T H_{i,j}^1 S_i, \check{M}_{i,j}^1 = S_i^T M_{i,j}^1 S_i, \nu \in \{1, 2\}$ . Pre- and post-multiplying inequality (50) by  $\text{diag}\{S_j^{-1}, S_j^{-1}, S_j^{-1}, S_j^{-1}, S_j^{-1}, I, S_j^{-1}, I, I, I\}$  and its transpose respectively,  $-\check{M}_{i,j}^{-1} \leq \check{M}_{i,j}^1 - 2S_j, -\check{M}_{i,j}^{-2} \leq \check{M}_{i,j}^2 - 2S_j, -\check{D}_{i,j}^{-1} \leq \check{D}_{i,j} - 2S_j$ , and Schur's formula, we can obtain

$$\begin{bmatrix} \check{\Xi}_{11} & \check{\Xi}_{12} \\ * & \check{\Xi}_{22} \end{bmatrix} < 0, \tag{74}$$

where

$$\check{\Xi}_{12} = \begin{bmatrix} \mathbf{0} & \mathbf{0} \\ \varepsilon_m A_i^T & (\varepsilon_M - \varepsilon_m) A_i^T \\ \varepsilon_m K_j^T \tilde{B}_i^T & (\varepsilon_M - \varepsilon_m) K_j^T \tilde{B}_i^T \\ \mathbf{0} & \mathbf{0} \\ \mathbf{0} & \mathbf{0} \\ \varepsilon_m E_i & (\varepsilon_M - \varepsilon_m) E_i \\ -\varepsilon_m K_j^T \tilde{B}_i^T & -(\varepsilon_M - \varepsilon_m) K_j^T \tilde{B}_i^T \\ \mathbf{0} & \mathbf{0} \end{bmatrix}, \tag{75}$$

$$\check{\Xi}_{22} = \text{diag}\{-M_{i,j}^{-1}, -M_{i,j}^{-2}\}. \tag{76}$$

With the Schur complement, inequality (74) can be transformed into

$$\Xi + \gamma_1^T S_j \gamma_2 + \gamma_2^T S_j^T \gamma_1 < 0, \tag{77}$$

where

$$\Xi = \begin{bmatrix} \check{\Xi}_3 & \check{\Xi}_5 \\ * & \check{\Xi}_{22} \end{bmatrix}, \tag{78}$$

$$\check{\Xi}_5 = \begin{bmatrix} \mathbf{0} & \mathbf{0} \\ \varepsilon_m A_i^T & (\varepsilon_M - \varepsilon_m) A_i^T \\ \varepsilon_m K_j^T \tilde{B}_i^T & (\varepsilon_M - \varepsilon_m) K_j^T \tilde{B}_i^T \\ \mathbf{0} & \mathbf{0} \\ \mathbf{0} & \mathbf{0} \\ \varepsilon_m E_i & (\varepsilon_M - \varepsilon_m) E_i \\ -\varepsilon_m K_j^T \tilde{B}_i^T & -(\varepsilon_M - \varepsilon_m) K_j^T \tilde{B}_i^T \end{bmatrix}, \tag{79}$$

$$\tilde{\mathbf{U}}_{11} = \begin{bmatrix} -\mathbf{S}_i - \mathbf{S}_i^T & \mathbf{A}_i \mathbf{S}_i + \tilde{\mathbf{P}}_i & \tilde{\mathbf{B}}_i \mathbf{Y}_i & \mathbf{0} & \mathbf{0} & \mathbf{E}_i & -\tilde{\mathbf{B}}_i \mathbf{Y}_i & \mathbf{0} \\ * & \tilde{\mathbf{U}}_{01} & \mathbf{0} & \tilde{\mathbf{M}}_i^1 & \mathbf{0} & \mathbf{0} & \mathbf{0} & \mathbf{0} \\ * & * & \tilde{\mathbf{U}}(33) & \tilde{\mathbf{U}}(34) & \tilde{\mathbf{U}}(35) & \mathbf{0} & \mathbf{0} & \mathbf{Y}_i^T \\ * & * & * & \tilde{\mathbf{U}}(44) & e^{\alpha_i \varepsilon_m} \tilde{\mathbf{Z}}_i & \mathbf{0} & \mathbf{0} & \mathbf{0} \\ * & * & * & * & \tilde{\mathbf{U}}(55) & \mathbf{0} & \mathbf{0} & \mathbf{0} \\ * & * & * & * & * & -\mathbf{I} & \mathbf{0} & \mathbf{0} \\ * & * & * & * & * & * & -\tilde{\Phi}_i & -\mathbf{Y}_i^T \\ * & * & * & * & * & * & * & \tilde{\mathbf{D}}_i - 2\mathbf{S}_i \end{bmatrix}. \quad (55)$$

$$\tilde{\mathbf{U}}_0 = \begin{bmatrix} -\mathbf{S}_j - \mathbf{S}_j^T & \mathbf{A}_i \mathbf{S}_j + \tilde{\mathbf{P}}_{i,j} & \tilde{\mathbf{B}}_i \mathbf{Y}_j & \mathbf{0} & \mathbf{0} & \mathbf{E}_i & -\tilde{\mathbf{B}}_i \mathbf{Y}_j & \mathbf{0} \\ * & \tilde{\mathbf{E}}_{01} & \mathbf{0} & \tilde{\mathbf{M}}_{i,j}^1 & \mathbf{0} & \mathbf{0} & \mathbf{0} & \mathbf{0} \\ * & * & \tilde{\mathbf{E}}(33) & \tilde{\mathbf{E}}(34) & \tilde{\mathbf{E}}(35) & \mathbf{0} & \mathbf{0} & \mathbf{Y}_j^T \\ * & * & * & \tilde{\mathbf{E}}(44) & e^{\gamma_{i,j} \varepsilon_m} \tilde{\mathbf{Z}}_{i,j} & \mathbf{0} & \mathbf{0} & \mathbf{0} \\ * & * & * & * & \tilde{\mathbf{E}}(55) & \mathbf{0} & \mathbf{0} & \mathbf{0} \\ * & * & * & * & * & -\mathbf{I} & \mathbf{0} & \mathbf{0} \\ * & * & * & * & * & * & -\tilde{\Phi}_j & -\mathbf{Y}_j^T \\ * & * & * & * & * & * & * & \tilde{\mathbf{D}}_{i,j} - 2\mathbf{S}_j \end{bmatrix}. \quad (58)$$

$$\tilde{\mathbf{U}}_{11} = \begin{bmatrix} -\mathbf{X}_j - \mathbf{X}_j^T & \mathbf{X}_j \mathbf{A}_i + \mathbf{P}_{i,j} & \mathbf{X}_j^T \tilde{\mathbf{B}}_i \mathbf{K}_j & \mathbf{0} & \mathbf{0} & \mathbf{X}_j \mathbf{E}_i & -\mathbf{X}_j^T \tilde{\mathbf{B}}_i \mathbf{K}_j & \mathbf{0} \\ * & \tilde{\mathbf{E}}_{01} & \mathbf{0} & \tilde{\mathbf{M}}_{i,j}^1 & \mathbf{0} & \mathbf{0} & \mathbf{0} & \mathbf{0} \\ * & * & \mathbf{\Xi}(22) & \mathbf{\Xi}(23) & \mathbf{\Xi}(24) & \mathbf{0} & \mathbf{0} & \mathbf{K}_j^T \\ * & * & * & \mathbf{\Xi}(33) & e^{\gamma_{i,j} \varepsilon_m} \mathbf{Z}_{i,j} & \mathbf{0} & \mathbf{0} & \mathbf{0} \\ * & * & * & * & \mathbf{\Xi}(44) & \mathbf{0} & \mathbf{0} & \mathbf{0} \\ * & * & * & * & * & -\mathbf{I} & \mathbf{0} & \mathbf{0} \\ * & * & * & * & * & * & -\tilde{\Phi}_j & -\mathbf{K}_j^T \\ * & * & * & * & * & * & * & -\mathbf{D}_{i,j}^{-1} \end{bmatrix}. \quad (73)$$

$$\tilde{\mathbf{E}}_3 = \begin{bmatrix} \mathbf{0} & \mathbf{P}_{i,j} & \mathbf{0} & \mathbf{0} & \mathbf{0} & \mathbf{0} & \mathbf{0} \\ * & \tilde{\mathbf{E}}_{01} & \mathbf{0} & \mathbf{M}_{i,j}^1 & \mathbf{0} & \mathbf{0} & \mathbf{0} \\ * & * & \mathbf{\Xi}(22) & \mathbf{\Xi}(23) & \mathbf{\Xi}(24) & \mathbf{0} & \mathbf{0} \\ * & * & * & \mathbf{\Xi}(33) & e^{\gamma_{i,j} \varepsilon_m} \mathbf{Z}_{i,j} & \mathbf{0} & \mathbf{0} \\ * & * & * & * & \mathbf{\Xi}(44) & \mathbf{0} & \mathbf{0} \\ * & * & * & * & * & -\mathbf{I} & \mathbf{0} \\ * & * & * & * & * & * & -\tilde{\Phi}_j \end{bmatrix}, \quad (80)$$

$$\tilde{\mathbf{E}}_{01} = -\gamma_{i,j} \mathbf{P}_{i,j} + \mathbf{H}_{i,j}^1 - \mathbf{M}_{i,j}^1 + \mathbf{Q}_{i,j}, \quad (81)$$

$$\mathbf{Y}_1 = [ \mathbf{I} \quad \mathbf{A}_i \quad \tilde{\mathbf{B}}_i \mathbf{K}_j \quad \mathbf{0} \quad \mathbf{0} \quad \mathbf{E}_i \quad -\tilde{\mathbf{B}}_i \mathbf{K}_j \quad \mathbf{0} \quad \mathbf{0} ], \quad (82)$$

$$\mathbf{Y}_2 = [ \mathbf{I} \quad \mathbf{0} \quad \mathbf{0} \quad \mathbf{0} \quad \mathbf{0} \quad \mathbf{0} \quad \mathbf{0} \quad \mathbf{0} \quad \mathbf{0} ]. \quad (83)$$

Multiply the left and right sides of inequality (77) by  $\tilde{\mathbf{R}} = [\mathbf{R}_1^T \quad \mathbf{I}_{8 \times 8}]$  and its transpose respectively, to obtain

$$\tilde{\mathbf{R}}^T (\mathbf{\Xi} + \mathbf{Y}_1^T \mathbf{S}_j \mathbf{Y}_2 + \mathbf{Y}_2^T \mathbf{S}_j^T \mathbf{Y}_1) \tilde{\mathbf{R}} < \mathbf{0}, \quad (84)$$

where  $\tilde{\mathbf{R}}_1 = [\mathbf{A}_i, \tilde{\mathbf{B}}_i \mathbf{K}_j, \mathbf{0}, \mathbf{0}, \mathbf{E}_i, -\tilde{\mathbf{B}}_i \mathbf{K}_j, \mathbf{0}, \mathbf{0}]$ . From inequality (84), we can derive that  $\tilde{\mathbf{R}}^T \mathbf{\Xi} \tilde{\mathbf{R}} < \mathbf{0}$ , which means that inequality (50) shows that inequality (12) is correct. Similarly, inequality (49) means that inequality (11) is correct. Pre- and post-multiplying inequality (51) by  $\text{diag}\{\mathbf{S}_i^{-1}, \mathbf{S}_i^{-1}\}$  and its transpose respectively, inequality (13) is obtained. Similarly, from inequality (14) we obtain inequality (52). Then, combined with inequalities (53) and (54), the inequality conditions (inequalities (15) and (16)) are constructed. Hence, based on inequalities (18) and (49)–(54), guaranteed cost control of system (5) is proven to be feasible.

### 4 Simulation

An example is given to prove the effectiveness of the proposed method. Fig. 2 shows the buck-boost



voltage circuit. The mathematical model expression is

$$\begin{cases} \dot{i}_L = \frac{\eta_1}{L}v_i - \frac{\eta_2}{L}v_0, \\ \dot{v}_0 = \frac{\eta_1}{C}i_L - \frac{\eta_2}{CR}v_0 - \frac{1}{C}i_l, \end{cases} \quad (85)$$

where  $v_0$  is the output voltage,  $i_l$  is the current source load as the disturbance term,  $i_L$  is the inductor current, and  $\eta_1$  and  $\eta_2$  are the duty cycles of  $S_1$  and  $S_2$ , respectively. For  $\sigma(t) \in \{1, 2\}$ , Eq. (85) is equivalent to

$$\dot{\mathbf{x}}(t) = \mathbf{A}_{\sigma(t)}\mathbf{x}(t) + \mathbf{B}_{\sigma(t)}\mathbf{u}(t), \quad (86)$$

where  $\mathbf{x} = [i_L \ v_0]^T$  and  $\mathbf{u} = [v_i \ i_l]^T$ .

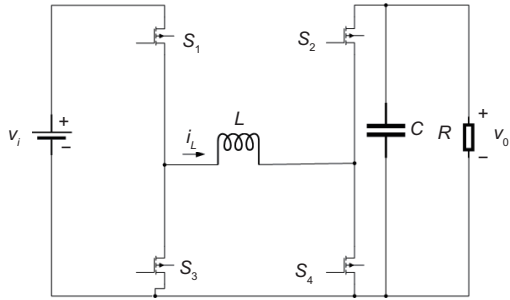


Fig. 2 Buck-boost voltage circuit

- (1)  $\eta_1 = 0.5, \eta_2 = 0,$

$$\mathbf{A}_1 = \begin{bmatrix} 0 & -\frac{\eta_2}{L} \\ \frac{\eta_1}{C} & -\frac{\eta_2}{CR} \end{bmatrix}, \mathbf{B}_1 = \begin{bmatrix} \frac{\eta_1}{L} & 0 \\ 0 & -\frac{1}{C} \end{bmatrix};$$

- (2)  $\eta_1 = 0.5, \eta_2 = 0.5,$

$$\mathbf{A}_2 = \begin{bmatrix} 0 & -\frac{\eta_2}{L} \\ \frac{\eta_1}{C} & -\frac{\eta_2}{CR} \end{bmatrix}, \mathbf{B}_2 = \begin{bmatrix} \frac{\eta_1}{L} & 0 \\ 0 & -\frac{1}{C} \end{bmatrix}.$$

By setting  $R = 0.5 \ \Omega, L = 1 \ \text{H}, C = 1 \ \text{F},$  and  $v_i = 50 \ \text{V},$  we can obtain

$$\mathbf{A}_1 = \begin{bmatrix} 0 & 0 \\ 0.5 & 0 \end{bmatrix}, \quad \mathbf{B}_1 = \begin{bmatrix} 0.5 & 0 \\ 0 & -1 \end{bmatrix},$$

$$\mathbf{A}_2 = \begin{bmatrix} 0 & -0.5 \\ 0.5 & -1 \end{bmatrix}, \quad \mathbf{B}_2 = \begin{bmatrix} 0.5 & 0 \\ 0 & -1 \end{bmatrix},$$

and assume that the other matrices of the system are

$$\mathbf{E}_1 = \begin{bmatrix} 2.55 & 0 \\ 0 & -1.02 \end{bmatrix}, \quad \mathbf{E}_2 = \begin{bmatrix} 0.34 & 0 \\ 0 & -1.03 \end{bmatrix}.$$

Let  $c_1 = 0.05, c_2 = 2, T_f = 12, h = 0.02, d = 0.002, N_0 = 0, \partial_1 = \partial_2 = 0.002, \varepsilon_m = 0.21, \varepsilon_M = 0.5,$

$\alpha_1 = 0.56, \alpha_2 = 0.42.$  By solving condition (49) in Theorem 2, the values of  $\mathbf{S}_i$  and  $\mathbf{Y}_i$  can be found. Then, combined with  $\mathbf{Y}_i = \mathbf{K}_i\mathbf{S}_i,$  we can determine the controller gains

$$\mathbf{K}_1 = \begin{bmatrix} 0.1281 & -0.0163 \\ -0.0247 & 0.2114 \end{bmatrix},$$

$$\mathbf{K}_2 = \begin{bmatrix} 0.1196 & 0.0292 \\ 0.0093 & 0.1757 \end{bmatrix},$$

and the event-triggered matrices

$$\Phi_1 = \begin{bmatrix} 0.2715 & -0.0296 \\ -0.0296 & 0.2635 \end{bmatrix},$$

$$\Phi_2 = \begin{bmatrix} 0.1892 & 0.0045 \\ 0.0045 & 0.1911 \end{bmatrix}.$$

Table 1 shows the waveform diagrams corresponding to the stable and unstable situations of the system over asynchronous finite-time intervals, along with matrix  $\mathbf{A}_{i,j}$  and parameters  $\mu_{i,j}$  and  $\gamma_{i,j}.$  From Table 1, we can see that  $\mathbf{A}_{2,1} = \mathbf{A}_2 + \mathbf{B}_2\mathbf{K}_1$  is finite-time stable (Fig. b), while  $\mathbf{A}_{1,2} = \mathbf{A}_1 + \mathbf{B}_1\mathbf{K}_2$  is finite-time unstable (Fig. a), which satisfies  $0 < \mu_{2,1} < 1, \gamma_{2,1} > 0$  and  $\mu_{1,2} > 1, \gamma_{1,2} < 0,$  respectively.

Select the disturbance  $\omega(t) = [e^{-t} \sin t, e^{-t} \sin t]$  and the initial value  $\mathbf{x}(0) = [0.91, 0.93]^T.$  Fig. 3 shows the periodic switching path under the asynchronous switching  $\overset{1^{\text{st}}}{1} \rightarrow \overset{2^{\text{nd}}}{2} \rightarrow \overset{1^{\text{st}}}{1} \rightarrow \overset{2^{\text{nd}}}{2} \rightarrow \dots.$  The released intervals of the ETS under AED-ADT are displayed in Fig. 4.

Under asynchronous switching, the response of  $\mathbf{x}^T(t)\mathbf{R}\mathbf{x}(t)$  combined with slow AED-ADT

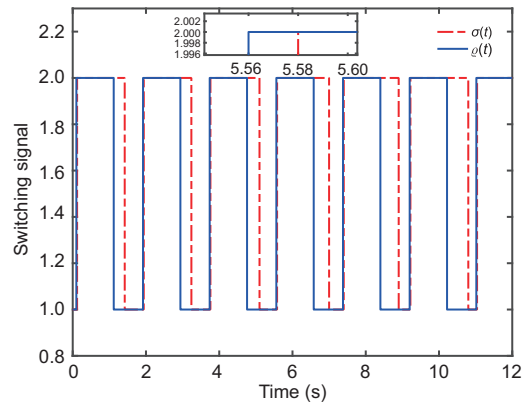
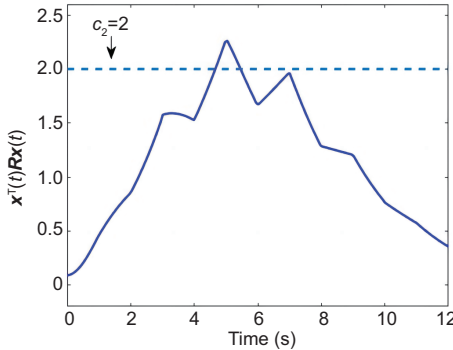
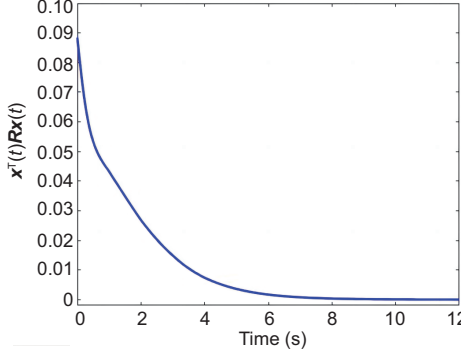
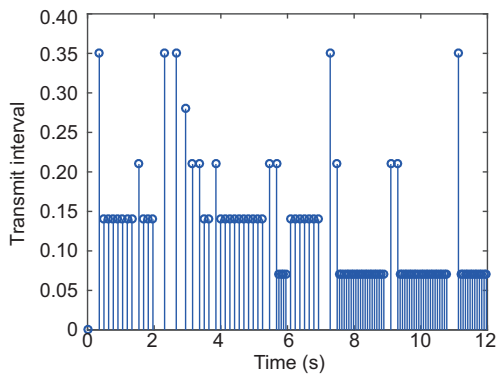


Fig. 3 Asynchronous switching signal based on admissible edge-dependent average dwell time (AED-ADT) switching

**Table 1** Matrix  $A_{i,j} \triangleq A_i + B_i K_j$  and parameters  $v_{i,j}$ ,  $\mu_{i,j}$ ,  $\gamma_{i,j}$ ,  $(\tau_{i,j}^a)^*$ ,  $(d_{i,j}^a)^*$

Matrix $A_{i,j}$	$A_{1,2}$	$A_{2,1}$
Graph		
	Fig. a	Fig. b
$v_{i,j}$	0.53	0.60
$\mu_{i,j}$	1.25	0.13
$\gamma_{i,j}$	-1.8	3.7
$(\tau_{i,j}^a)^*$	0.3873	0.7715
$(d_{i,j}^a)^*$	0.1177	0.2416



**Fig. 4** Intervals of release for the hybrid event-triggered scheme (HETS)

switching when the system is finite-time stable and with fast AED-ADT switching when the system is finite-time unstable is shown in Fig. 5.

Therefore, the switched system (5) is FTB with guaranteed cost performance index  $J^* = 0.2709$ . Fig. 6 shows that the response of  $x^T(t)Rx(t)$  with slow AED-ADT switching is adopted in finite-time stable and finite-time unstable situations of the asynchronous switching system.

**Remark 8** Table 1 shows that in the finite-time asynchronous interval, Fig. a is finite-time unstable; that is, controller  $\tilde{u}_l(t) = \Lambda_{l_t} K_2 x(g_r h)$  cannot stabilize subsystem 1, and we use the method of fast AED-ADT switching ( $\mu_{1,2} = 1.25 > 1, \gamma_{1,2} = -1.8$ ). In addition, Fig. b is finite-time stable;

that is, controller  $\tilde{u}_l(t) = \Lambda_{l_t} K_1 x(g_r h)$  can stabilize subsystem 2, and we use the method of slow AED-ADT switching ( $0 < \mu_{2,1} = 0.13 < 1, \gamma_{2,1} = 3.7$ ).

**Remark 9** From inequalities (18)–(20), it can be inferred that slow AED-ADT in the synchronous switching interval can be calculated using inequality (18), while slow AED-ADT and fast AED-ADT in the asynchronous interval can be calculated from inequalities (19) and (20), respectively. For system (86), which includes finite-time unstable subsystems (as shown in Table 1), to demonstrate the effectiveness of employing the fast–slow AED-ADT mixed switching strategy within the asynchronous interval, the method of controlling variables was used during the simulation process. When other parameters are kept unchanged and the system is finite-time stable within the asynchronous switching interval, fast AED-ADT is employed with  $d_{1,2}^a = 0.02$ , as shown in the response diagram of  $x^T(t)Rx(t)$  in Fig. 5. Conversely, when the system is finite-time unstable within the asynchronous switching interval, slow AED-ADT is used with  $d_{1,2}^a = 0.2$ , with the response diagrams of  $x^T(t)Rx(t)$  depicted in Fig. 6. By comparing Figs. 5 and 6, it can be seen that when the system is unstable in the asynchronous switching interval, the fast AED-ADT method has better response than the slow AED-ADT method. Therefore, the superiority of the fast–slow AED-ADT mixed switching strategy is further verified.

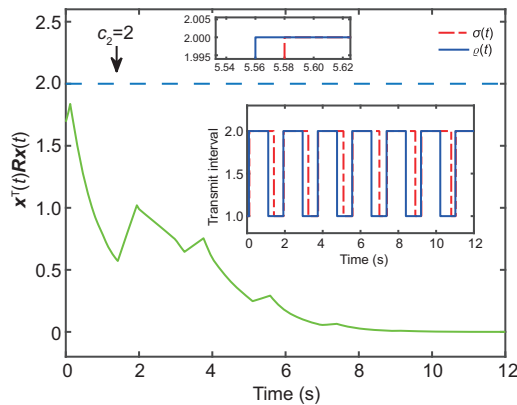


Fig. 5 Response of  $x^T(t)Rx(t)$  with inequalities (18) and (20)

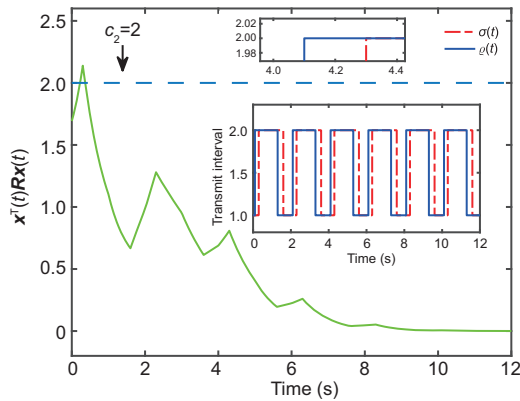


Fig. 6 Response of  $x^T(t)Rx(t)$  with inequalities (18) and (19)

## 5 Conclusions

This paper has studied the finite-time boundedness and guaranteed cost control of switched linear systems with asynchronous switching. By using ETS and RRP, the transmission of redundant information is reduced and the sensor's permission to receive data is more practical, thus easing the bandwidth pressure. The design of the switching signal adopts the AED-ADT method, including slow and fast AED-ADT. In this switching signal, the maximum delay limit for asynchronous switching is eliminated. By constructing the Lyapunov function related to the system mode and the controller mode, the controller gain and finite-time bounded criteria of the controlled switched system are obtained. Finally, the validity of the obtained results is verified by an example. In the process of network communication, the system is easily attacked. Therefore, in future research, denial-of-service attack will be incor-

porated into the proposed method to further reduce the conservatism of the system.

## Contributors

Hangli REN, Qingxi FAN, and Linlin HOU designed the research. Hangli REN processed the data and drafted the paper. Qingxi FAN helped organize the paper. Hangli REN and Linlin HOU revised and finalized the paper.

## Conflict of interest

All the authors declare that they have no conflict of interest.

## Data availability

The data that support the findings of this study are available from the corresponding author upon reasonable request.

## References

- Amini A, Asif A, Mohammadi A, et al., 2021. Sampled-data dynamic event-triggering control for networked systems subject to DoS attacks. *IEEE Trans Netw Sci Eng*, 8(3):1978-1990. <https://doi.org/10.1109/TNSE.2021.3070804>
- Branicky MS, 1998. Multiple Lyapunov functions and other analysis tools for switched and hybrid systems. *IEEE Trans Automat Contr*, 43(4):475-482. <https://doi.org/10.1109/9.664150>
- Dorf R, Farren M, Phillips C, 1962. Adaptive sampling frequency for sampled-data control systems. *IRE Trans Automat Contr*, 7(1):38-47. <https://doi.org/10.1109/TAC.1962.1105415>
- Du SL, Dong JT, Li X, et al., 2022. Stability and stabilization for switched positive systems under a weighted MDADT method. *J Franklin Inst*, 359(8):3656-3670. <https://doi.org/10.1016/j.jfranklin.2022.03.001>
- Gao LJ, Cao ZB, Zhang M, et al., 2020. Input-to-state stability for hybrid delayed systems with admissible edge-dependent switching signals. *J Franklin Inst*, 357(13):8823-8850. <https://doi.org/10.1016/j.jfranklin.2020.06.008>
- Hu J, Wang ZD, Chen DY, et al., 2016. Estimation, filtering and fusion for networked systems with network-induced phenomena: new progress and prospects. *Inform Fusion*, 31:65-75. <https://doi.org/10.1016/j.inffus.2016.01.001>
- Huang J, Ma X, Che HC, et al., 2020. Further result on interval observer design for discrete-time switched systems and application to circuit systems. *IEEE Trans Circ Syst II Exp Briefs*, 67(11):2542-2546. <https://doi.org/10.1109/TCSII.2019.2957945>
- Karamanakos P, Nahalparvari M, Geyer T, 2021. Fixed switching frequency direct model predictive control with continuous and discontinuous modulation for grid-tied converters with LCL filters. *IEEE Trans Contr Syst Technol*, 29(4):1503-1518. <https://doi.org/10.1109/tcst.2020.3008030>

- Li DH, Liang JL, Wang F, 2020. Observer-based output feedback  $H_\infty$  control of two-dimensional systems with periodic scheduling protocol and redundant channels. *IET Contr Theory Appl*, 14(20):3713-3722. <https://doi.org/10.1049/iet-cta.2020.0590>
- Liu K, Fridman E, Johansson KH, 2015. Networked control with stochastic scheduling. *IEEE Trans Automat Contr*, 60(11):3071-3076. <https://doi.org/10.1109/TAC.2015.2414812>
- Liu SL, Niu B, Zong GD, et al., 2022. Adaptive fixed-time hierarchical sliding mode control for switched under-actuated systems with dead-zone constraints via event-triggered strategy. *Appl Math Comput*, 435:127441. <https://doi.org/10.1016/j.amc.2022.127441>
- Mao JY, Sun Y, Yi X, et al., 2021. Recursive filtering of networked nonlinear systems: a survey. *Int J Syst Sci*, 52(6):1110-1128. <https://doi.org/10.1080/00207721.2020.1868615>
- Merlin GB, Moreira LG, da Silva JM Jr, 2021. Periodic event-triggered control for linear systems in the presence of cone-bounded nonlinear inputs: a discrete-time approach. *J Contr Autom Electr Syst*, 32(1):42-56. <https://doi.org/10.1007/s40313-020-00645-1>
- Murugesan S, Liu YC, 2019. Resilient memory event-triggered finite-time bounded for networked control systems with multiple cyber-attacks. *American Control Conf*, p.2713-2719. <https://doi.org/10.23919/ACC50511.2021.9482984>
- Murugesan S, Liu YC, 2022. Finite-time resilient control for networked control systems with multiple cyber-attacks: memory/adaptive event-triggered scheme. *Int J Adapt Contr Signal Process*, 36(4):901-925. <https://doi.org/10.1002/acs.3379>
- Qi YW, Zeng PY, Bao W, 2018. Event-triggered and self-triggered  $H_\infty$  control of uncertain switched linear systems. *IEEE Trans Syst Man Cybern Syst*, 50(4):1442-1454. <https://doi.org/10.1109/TSMC.2018.2801284>
- Qi YW, Liu YH, Fu J, et al., 2019. Event-triggered  $L_\infty$  control for network-based switched linear systems with transmission delay. *Syst Contr Lett*, 134:104533. <https://doi.org/10.1016/j.sysconle.2019.104533>
- Shang H, Zong GD, Shi KB, 2022. Neural-network-based distributed security filtering for networked switched systems. *Int J Robust Nonl Contr*, 32(5):2791-2804. <https://doi.org/10.1002/rnc.5554>
- Sun YR, Sun YG, Yang CZ, 2021. Finite-time control of networked control systems with time delay and packet dropout. *J Contr Sci Eng*, 2021(1):3093865. <https://doi.org/10.1155/2021/3093865>
- Wakaiki M, Sano H, 2019. Stability analysis of infinite-dimensional event-triggered and self-triggered control systems with Lipschitz perturbations. <https://arxiv.org/abs/1911.12916>
- Wan XB, Wang ZD, Wu M, et al., 2019.  $H_\infty$  state estimation for discrete-time nonlinear singularly perturbed complex networks under the round-robin protocol. *IEEE Trans Neur Netw Learn Syst*, 30(2):415-426. <https://doi.org/10.1109/TNNLS.2018.2839020>
- Wang D, Wang ZD, Shen B, et al., 2019.  $H_\infty$  finite-horizon filtering for complex networks with state saturations: the weighted try-once-discard protocol. *Int J Robust Nonl Contr*, 29(7):2096-2111. <https://doi.org/10.1002/rnc.4479>
- Wang WJ, Xu D, Zhou JP, et al., 2023. Cost-guaranteed exponential stabilization of Lurie systems via switched event-triggered control. *Discret Contin Dyn Syst-Ser B*, 28(4):2828-2845. <https://doi.org/10.3934/dcdsb.2022194>
- Wang YD, Zong GD, Yang D, et al., 2022. Finite-time adaptive tracking control for a class of nonstrict feedback nonlinear systems with full state constraints. *Int J Robust Nonl Contr*, 32(5):2551-2569. <https://doi.org/10.1002/rnc.5777>
- Weiss L, Infante EF, 1965. On the stability of systems defined over a finite time interval. *Proc Natl Acad Sci USA*, 54(1):44-48. <https://doi.org/10.1073/pnas.54.1.44>
- Wen GH, Wan Y, Cao JD, et al., 2016. Master-slave synchronization of heterogeneous systems under scheduling communication. *IEEE Trans Syst Man Cybern Syst*, 48(3):473-484. <https://doi.org/10.1109/TSMC.2016.2599012>
- Xiang WM, Johnson TT, 2017. Event-triggered control for continuous-time switched linear systems. *IET Contr Theory Appl*, 11(11):1694-1703. <https://doi.org/10.1049/iet-cta.2016.0672>
- Xie HZ, Zong GD, Bu W, et al., 2022. Input-to-state practical stability of switched affine systems with time-varying delay: an event-triggered mechanism. *Int J Syst Sci*, 53(9):1983-1994. <https://doi.org/10.1080/00207721.2022.2031341>
- Xu N, Liu X, Li YL, et al., 2024. Dynamic event-triggered control for a class of uncertain strict-feedback systems via an improved adaptive neural networks backstepping approach. *IEEE Trans Autom Sci Eng*, early access. <https://doi.org/10.1109/TASE.2024.3374522>
- Yang JQ, Zhao XD, Bu XH, et al., 2018. Stabilization of switched linear systems via admissible edge-dependent switching signals. *Nonl Anal Hybrid Syst*, 29:100-109. <https://doi.org/10.1016/j.nahs.2018.01.003>
- Yang L, Guan CX, Fei ZY, 2019. Finite-time asynchronous filtering for switched linear systems with an event-triggered mechanism. *J Franklin Inst*, 356(10):5503-5520. <https://doi.org/10.1016/j.jfranklin.2019.03.019>
- Zou L, Wang ZD, Gao HJ, et al., 2017. Finite-horizon  $H_\infty$  consensus control of time-varying multiagent systems with stochastic communication protocol. *IEEE Trans Cybern*, 47(8):1830-1840. <https://doi.org/10.1109/TCYB.2017.2685425>

## List of supplementary materials

Proof of Theorem 1